

# Compressed Parametric and Non-Parametric Approximations to the Gravitational Wave Likelihood

V. Delfavero,<sup>1,\*</sup> R. O’Shaughnessy,<sup>2</sup> D. Wysocki,<sup>3</sup> and A. Yelikar<sup>2</sup>

<sup>1</sup>*NASA Postdoctoral Program, Astrophysics Science Division, NASA Goddard Space Flight Center, Greenbelt, MD 20771, USA*

<sup>2</sup>*Center for Computational Relativity and Gravitation, Rochester Institute of Technology, Rochester, New York 14623, USA*

<sup>3</sup>*Department of Physics, University of Wisconsin–Milwaukee, Milwaukee, WI 53201, USA*

(Dated: December 8, 2022)

Gravitational-wave observations of quasicircular compact binary mergers imply complicated posterior measurements of their parameters. Though Gaussian approximations to the pertinent likelihoods have decades of history in the field, the relative generality and practical utility of these approximations hasn’t been appreciated, given focus on careful, comprehensive generic Bayesian parameter inference. Building on our previous work in three dimensions, we demonstrate by example that bounded multivariate normal likelihood approximations are a sufficiently accurate representation of the full likelihood of observed gravitational-wave sources. Fits for each event are published in the Gravitational-Wave Transient Catalogs at <https://gitlab.com/xevra/nal-data>, along with a code release at <https://gitlab.com/xevra/gwalk>. We argue our approximations are more than accurate enough for population inference and introduce much smaller errors than waveform model systematics. To demonstrate the utility of these approximations as parametric models for the likelihood of individual gravitational-wave sources, we show examples of their application to modeling the population of observed gravitational-wave sources as well as low-latency parameter inference.

## I. INTRODUCTION

The first gravitational-wave observation was made by the Laser Interferometer Gravitational-wave Observatory (LIGO) in 2015 [2, 3, 8]. To date, the LIGO Scientific Collaboration, together with VIRGO and KAGRA, have reported the detection of 90 gravitational-wave signals from merging compact binaries in the Gravitational-Wave Transient Catalogs [4, 6, 7, 9, 13, 32, 34]. Many groups have developed non-LVK catalogs, and while important, they are not the focus of our study [22, 25, 62, 66, 82]. These merging compact binaries include Binary Black Hole (BBH), Binary Neutron Star (BNS), and Neutron-Star-Black-Hole (NSBH) mergers. As each observation is merely a strain signal identified in each interferometer, extracting information from these signals requires a Bayesian statistical inverse technique: gravitational-wave parameter estimation.

Many groups have developed methodology to evaluate the agreement of a gravitational-wave signal to relativistic waveform models in a space of these parameters [12, 20, 62, 74, 89, 109]. There is additional consideration for events which may have electromagnetic counterparts, and a low latency parameter estimation pipeline must identify and localize such detections [1, 29, 39, 48, 50, 78, 98]. These groups strive to yield fast and accurate parameter estimates for the parameters of each event. The parameters associated with a given binary can be split into *extrinsic* parameters which depend on the orientation of a source relative to the observer, and the *intrinsic* parameters which do not. The astrophysical parameters of interest to a study of the underlying

population of merging binaries include the intrinsic parameters and distance ( $d_L$ ). The intrinsic parameters of a binary black hole system (BBH) include the mass of each companion ( $m_i$ ) as well as the dimensionless spin ( $\chi_i$ ). For binary neutron star mergers, the tidal deformability of each companion ( $\Lambda_i$ ) is also estimated. Collectively, these are the astrophysical parameters ( $x$ ) of the compact binary merger. These describe a system without reference to the observer, and fully characterize the astrophysical properties of the underlying population of merging binaries.

Various methods are used to estimate various marginal likelihood functions for the astrophysical parameters of gravitational-wave events, after a standard Bayesian inference code has explored the full multidimensional posterior. [2, 28, 42, 54, 55, 67, 74]. These approximations enable us to better understand gravitational-wave sources, and perform hierarchical inference. These methods include nonparametric approximations such as RIFT [74], and sample-based estimates such as histograms and Kernel Density Estimates (KDEs) [54]. In practice, these methods may suffer from performance limitations and their own boundary condition limitations. Histograms in particular, face binning effects and a lack of smoothness. Better adapted non-parametric methods like carefully tuned Gaussian mixture models can significantly mitigate binning and smoothness effects; see e.g. [55] for an example with GW170817. The multivariate normal distribution, in particular, works well for describing the likelihood function for the astrophysical parameters of gravitational-wave events [2, 28, 67, 74]. A truncated set of samples can introduce bias in the standard method of implementing the multivariate normal distribution. Previously, we have introduced optimized fits for the bounded multivariate normal distribution in the aligned-spin case, which overcome this source of bias [41].

---

\* msd8070@rit.edu

In this work, we introduce high dimensional bounded (truncated) multivariate Normal Approximate Likelihood (NAL) models in order to fully characterize precessing spin degrees of freedom for gravitational-wave events, as well as tidal parameters for binary neutron star mergers. We provide a detailed algorithm and code to perform the necessary constrained high-dimensional optimization of pertinent Gaussian parameters. We apply our algorithm to the gravitational-wave events observed by LIGO-Virgo-Kagra in their first three observing runs, finding simple (truncated) Gaussian likelihoods for the astrophysical parameters of interest for each event, which we report in an associated data release.

Accurate Gaussian likelihood approximations have an enormous range of practical applications in gravitational-wave astrophysics. For example, because of their simplicity, they’re a compact and human-comprehensible expression of binary parameters. They’re also an extremely efficient to employ in large-scale population inference calculations, circumventing many problems associated with using finite sets of posterior samples (i.e., the “delta function” problem when a model avoids any sample; and more generally the voracious need for more samples from every event as observations are increasingly constraining). Furthermore, many groups are working to constrain astrophysical models such as the evolution of massive stellar binaries and the neutron star equation of state using methods such as Bayesian hierarchical inference [5, 19, 23, 24, 33, 42, 46, 51, 54, 55, 81, 95, 96, 100, 104, 106, 115–117]

Finally, truncated Gaussian approximations have immediate practical utility for low-latency parameter inference due to their swift evaluation and compact set of model parameters.

This paper is organized as follows. In section II, we describe the generation of the multivariate normal distribution from the LIGO catalog posterior samples, as well as the non-parametric Gaussian Process model. We justify their validity as approximations to the true likelihood describing an observation. In section III, we describe the properties of the likelihood models generated for each event. We summarize the immediate value of these models to other applications. Finally, we summarize the astrophysical consequences of our findings, and we infer properties of the underlying compact binary population in section V.

### A. The rationale behind a simple likelihood approximation

In brief, our rationale is that current sample-based methods have intrinsic limitations. Although detailed and accurate approximations exist, a Gaussian approximation is fast, easy to interpret, and can be made without sacrificing more information than is lost through waveform systematics (see Figure 4).

Many of the impactful science goals deduced from the

observed sample of gravitational wave observations can only be addressed by comparing the full sample of gravitational wave observations  $\{d_k\}$  to a (parametric) population model, which predicts the properties  $x$  of individual sources as random realizations of a population model  $p(x|\Lambda)$  where  $\Lambda$  are population model parameters. The consistency of any one gravitational wave observation and this population model can be quantified by a single-event marginal likelihood  $\ell_k(\Lambda) = \int dx \mathcal{L}_k(x)p(x|\Lambda)$ , where the likelihood  $\mathcal{L}_k(x) \propto p(d_k|x)$  quantifies the probability that the observed data  $d_k$  is consistent with Gaussian noise plus a single merger signal with parameters  $x$ . However, gravitational wave parameter inference results are currently usually characterized by discrete samples: fair draws from the posterior distribution  $\propto \mathcal{L}_x(x)p(x)$  for some fiducial prior [47]. Quantities like the marginal likelihood can be evaluated with these samples by reweighting; see, e.g., Appendix B in [114].

Unfortunately, many GW science objectives involve calculations where continuous inputs, not samples, might be preferable. These scenarios occur when the population model  $p(x|\Lambda)$  has sharp features, such as narrow subpopulation (e.g., black holes born with exactly zero spin, or neutron stars with a specific equation of state). When  $p(x|\Lambda)$  is very narrow, sample-based estimates for  $\ell_k$  break down [47, 49, 101]. Worse, as demonstrated by example Appendix B of [112], even ubiquitous spin prior reweighting can frequently introduce nominally infinite variance in pertinent Monte Carlo sums.

Fortunately, several techniques have been or are being developed to reconstruct the full GW likelihood, or more typically the likelihood marginalized over several nuisance parameters in  $x$  like the sky location and polarization. RIFT, the most well-developed, uses the marginal likelihood directly in its parameter inference [74, 85, 112], and the interpolated likelihood output has been directly used in EOS and population inference [11, 105, 117]; see also similar likelihood interpolation elsewhere for neutron stars [59]. Other groups are now prototyping methods to accurately reconstruct the likelihood overall [42, 55] and in limited circumstances [94].

Also, in early low-dimensional investigations using very few observable properties of  $x$ , many groups have adopted a dangerous kernel-density-estimate approach (e.g., [54, 73, 77, 94, 113]), attempting to reconstruct the single-event (marginal) likelihood over a small number of parameters simply by reweighting and smoothing the available samples. While viable for a handful of dimensions for typical sets of  $\simeq 10^4$  posterior samples, such an approach breaks down when working with the eight (for precessing binary black holes) to ten (for precessing binary neutron stars) dimensions required for generic sources. Aside from being fairly inaccurate and unable to capture many observations, these KDE-based methods are generally very slow, with computational cost scaling as the training data size.

A fast, easy-to-interpret approximation to the (marginal) likelihood  $\mathcal{L}$  will be useful exactly insofar as

it enables sufficiently accurate population inferences. To assess the threshold at which an approximation begins to bias our population estimates, we consider a one-observable toy model: a Gaussian population of binaries with parameter  $x$  (standard deviation  $\sigma_{\text{pop}}$ ), probed by Gaussian observations of  $x$  (standard deviation  $\sigma$ ). We will assume our approximate likelihood model introduces random measurement errors  $\delta x$  with zero mean and standard deviation  $\sigma_{\text{sys}}$ . In this model, we can measure the sample mean to be consistent with zero (e.g., by analogy to tests for zero average  $\chi_{\text{eff}}$ ) to an accuracy  $\sqrt{(\sigma_{\text{pop}}^2 + \sigma^2 + \sigma_{\text{sys}}^2)/N}$ . For this type of measurement, so long as the systematic error is small compared to both the population and individual measurement error, we'll still draw the conclusions about the average value of  $x$  with the same precision. Similarly, statements about the population width are only impacted if the systematic measurement error is comparable to or larger than the uncertainty in individual measurements or the population width. In short, unless dramatic, small random errors will usually average out.

More dangerous is the possibility that a likelihood approximation technique could be *consistently* biased (i.e., the mean of  $\delta x$  is not zero). For example, a likelihood approximation that was consistently but slightly biased against equal mass would, over time, produce evidence against all binaries being equal mass, even for a population of twins. To contaminate a population measurement with  $N$  observations, then, we would require a large bias of  $\langle \delta x \rangle > \sqrt{(\sigma_{\text{pop}}^2 + \sigma^2)/N}$ , equivalent to shifting the mean by of order  $1/\sqrt{N}$  standard deviations. For the near future, with only  $N \lesssim 10^3$  observations available, systematic biases smaller than the equivalent of a 3% shift in mean will be difficult to identify with population-level measurements, and then only if this hypothetical systematic produce a consistent impact one parameter for all events. [By contrast, waveform systematics often produces much larger differences, albeit in less-consistent parameter directions; see, e.g., [4, 7, 32, 34, 103].]

In this paper, we characterize distribution differences with the KL divergence  $D(p|q) = \int p \ln p/q dx$ . For two Gaussian distributions, a difference of  $\sigma/\sqrt{N}$  in the sample mean with minimal shift in variance corresponds to a KL divergence of  $1/2N$ . We therefore adopt  $1/2N$  as the most pessimistic scale for observationally-pertinent for KL divergences between observations, where  $N$  is a typical number of observations.

## II. METHODS

The multivariate normal distribution has long been used for gravitational-wave likelihood approximation [2, 27, 83, 84, 90]. However, many useful coordinates (such as mass ratio  $q$  and symmetric mass ratio  $\eta$ ), for which gravitational wave events are well parameterized, are affected by finite boundary effects. This causes a displace-

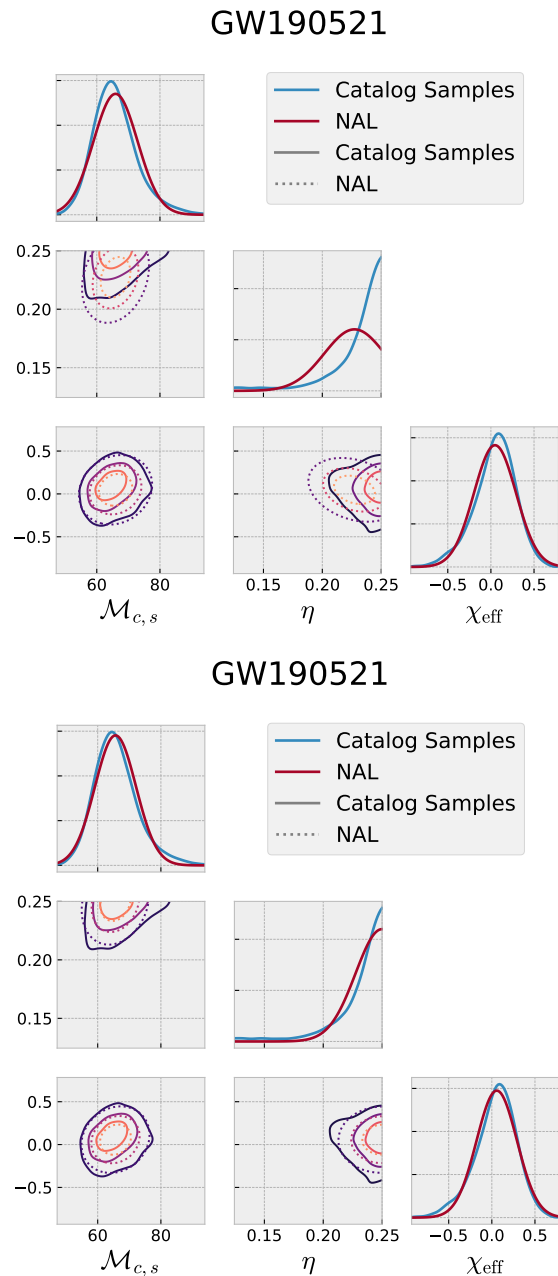


Figure 1. Multivariate normal likelihood approximation using two methods: (left) implicit parameterization and (right) optimized parameterization. Diagonal plots are one-dimensional marginalizations of the likelihood function, normalized on our bounded interval. Off-diagonal plots represent two-dimensional marginalizations, with contours drawn enclosing [25, 50, 75] confidence intervals. The Publication-Samples waveform samples for GW190521 are used for this example.

ment in the peak of the likelihood function from the mean or median of our parameter estimation samples (see Figure 1). By optimizing the parameters of the multivariate normal distribution, normalized on a finite interval, we

can overcome these limitations [41].

### A. Bayesian Inference

Using full numerical relativity to simulate precessing merger events is the only way to fully characterize a binary black hole inspiral and merger in complete rigor. While some groups are actively working on this [2, 16, 22, 25, 58, 60, 64, 66, 76, 79, 93, 119], computational limitations impose difficulties on such parameter estimation implementations [107]. The catalog associated with the first part of LIGO’s third observing run (O3a) explains that phenomenological, effective one body, and numerical relativity surrogate waveform approximants are used in place of direct numerical relativity parameter estimation for the Gravitational-wave Transient Catalogs [7]. We know that this posterior is the product  $\mathcal{L}(x) \times p(x)$ , where  $p(x)$  is a fiducial prior, and  $\mathcal{L}(x)$  is the marginal likelihood that a waveform with parameters  $x$  describes a real gravitational-wave observation. In this study we include likelihood approximations with the parameter estimation samples provided in the Gravitational-Wave Transient Catalogs [4, 7, 30–32, 34]. For each event in LIGO–Virgo’s third observing run, we provide Cartesian-spin models as well as aligned-spin models for each of the high modal waveforms available in the publicly released samples for each event. Waveforms included in the associated data release include IMRPhenomD [65, 69], IMRPhenomPv2 [56, 68], IMRPhenomPv3 [70], IMRPhenomPv3HM [86], IMRPhenomXPHM [53, 91, 92], SEOBNRv3 [88, 102], SEOBNRv4 [21], SEOBNRv4PHM [38, 87], and NRSur7dq4 [108] as well as others [10, 43, 44, 61, 80, 99].

Developing a likelihood approximation from posterior samples without revisiting gravitational-wave strain data requires re-weighting fair draw posterior samples by the inverse prior for each set of astrophysical parameters studied [17]. The mass prior removed from each posterior is uniform in detector component masses:

$$p(\mathcal{M}_{c,z}, \eta) d\mathcal{M}_{c,z} d\eta = \frac{4}{(M_{\max} - m_{\min})^2} \frac{\mathcal{M}_{c,z} d\mathcal{M}_{c,z} d\eta}{\eta^{6/5} \sqrt{1 - 4\eta}} \quad (1)$$

This is consistent with prior work [74]. The prior in spin removed for each posterior is uniform in Cartesian spin components [26]. For parameterizations which include a distance parameter, the prior removed is as the inverse square of the luminosity distance. A uniform prior is assumed for neutron star tidal parameters.

### B. Likelihood estimation

For parameters of which Gaussian noise is expected, but that face finite boundary constraints that significantly truncate a sampled distribution, direct inference of

the  $\mu$  and  $\Sigma$  parameters for a bounded multivariate normal distribution (from the sample mean and covariance) is a poor approximation. As with any parametric model, an alternate construction of  $\mu$  and  $\Sigma$  for a bounded multivariate normal distribution is to optimize those model parameters. This optimization compares the bounded multivariate normal distribution  $\mathcal{L}(\mathbf{x}|\mu, \Sigma) \propto G(\mathbf{x} - \mu, \Sigma)$  to an estimate of the marginalized sample distribution for each combination of one and two astrophysical parameters of interest (normalized on a bounded interval). To illustrate the effectiveness of this method, Figure 1 shows the benefit of an optimized fit visually. In that example for GW190521, the offset in  $\mu_\eta$  is  $1.006\sigma_\eta$  (from the optimized parameterization), where the marginals for the optimized method have an average KL divergence of 0.016, compared to the mean and covariance estimate’s 0.074. This demonstrates a clear increase in the optimized parameterization’s goodness of fit, over the simple inferred parameterization. More details about the estimation of this KL divergence statistic are included in Appendix B.

#### 1. Multivariate normal parameterization

The Multivariate Normal distribution has many properties which are ideal for population models, such as trivial normalization and ease of drawing fair-draw independent identically distributed random samples. The peak of the multivariate normal likelihood is characterized by a set of parameters  $\mu$ . Its shape is determined by a characteristic covariance  $\Sigma$ . The multivariate normal likelihood is given by

$$G(\mathbf{x} - \mu, \Sigma) = (|\pi\Sigma|)^{-\frac{1}{2}} \exp \left[ -\frac{1}{2}(\mathbf{x} - \mu)^T \Sigma^{-1}(\mathbf{x} - \mu) \right] \quad (2)$$

Values for each component of  $\mu$  and  $\Sigma$  can be inferred implicitly from the mean and covariance of a sample distribution. As seen in Figure 1, this has limitations when samples are affected by a finite boundary condition. We need to incorporate an assumption that our likelihood function  $\mathcal{L}(\mathbf{x}) \propto G(\mathbf{x} - \mu, \Sigma)$  inside of our bounded interval, and that  $\mathcal{L}(\mathbf{x}) = 0$  outside of that interval.

We optimize the multivariate normal distribution as a parametric model using maximum likelihood estimation (see appendix B). The characteristic covariance parameters can be further decomposed to reduce degeneracy in our model.  $\Sigma = \sigma\rho\sigma$ , where  $\sigma$  is a characteristic standard deviation, and  $\rho$  is a characteristic correlation matrix. The correlation parameters have useful properties of symmetry ( $\rho_{i,j} = \rho_{j,i}$ ), unity along the diagonal ( $\rho_{i,i} = 1$ ), and are bounded within  $-1 \leq \rho_{i,j} \leq 1$ . A multivariate normal distribution with  $k$  dimensions will have  $k$  parameters in  $\mu$ ,  $k$  parameters in  $\sigma$ , and  $(k^2 - k)/2$  parameters in  $\rho$ . These total  $(k^2 + 3k)/2$ .

A fully generic optimization of a parametric model describing the sample population would require an evaluation set  $\mathbf{X}_{eval}$  for the full dimensionality of our fit.

As the number of dimensions increases, the number of samples required would increase alongside it. At this stage, we take advantage of the fact that the multivariate normal distribution can be trivially marginalized to one- and two-dimensional marginals, without any loss of information. We fit all of the corresponding one- and two-dimensional marginals,  $G(x_i - \mu_i, \sigma_i)$  and  $G([x_i, x_j] - [\mu_i, \mu_j], [[\sigma_i^2, \sigma_i \sigma_j \rho_{ij}], [\sigma_i \sigma_j \rho_{ij}, \sigma_j^2]])$ , which are independently renormalized in their own bounded regions. In doing so, we also fit  $G(\mathbf{x} - \mu, \Sigma)$ .

The goodness of fit criterion for the NAL models are evaluated using a discretized Kullback-Leibler (KL) divergence, comparing the NAL approximation of  $\mathcal{L}(\mathbf{x})$  to that of the Gaussian process for each marginalization (see appendix B for more about error reduction) [72].

## 2. Non-parametric likelihood estimation

Optimizing the multivariate normal distribution as a parametric model benefits from an intermediate estimation of the marginal sample density. [The underlying reweighted posterior samples characterize a higher-dimensional posterior than the one we seek to model with a Gaussian, with many nuisance parameters; we do not simply fit a multivariate Gaussian applied to the whole the 15-dimensional posterior.] Instead, we use the fact that any multivariate Gaussian is fully determined by all of its one and two-dimensional Gaussian marginal distributions. With this general feature, we can reconstruct our multivariate Gaussian by comparing our Gaussian model to an estimated full marginal likelihood on these much simpler (and numerically very stable) lower-dimensional marginal distributions.

One set of methods for identifying these one- and two-dimensional marginal densities is to use histograms with various smoothing and binning procedures that reduce the risk of overfitting or underfitting a sample [97], and many of these solutions are used in gravitational-wave likelihood estimation [36, 37, 42, 75, 118]. We note that some of these works [42, 74] make use of Gaussian Process Regression to interpolate samples of the gravitational-wave likelihood function for individual events.

Motivated by these and other prior works, we use Gaussian-process approximations to our (reweighted) low-dimensional posterior histograms, to produce smooth intermediate non-parametric likelihood estimates for our one- and two-dimensional marginal distributions. Our implementation of Gaussian processes toward this objective makes use of one- and two-dimensional histograms with a fixed bin width; see Appendix B for details. These marginal fits provide a smooth interpolation of the likelihood function derived from the catalog samples, normalized on our bounded interval.

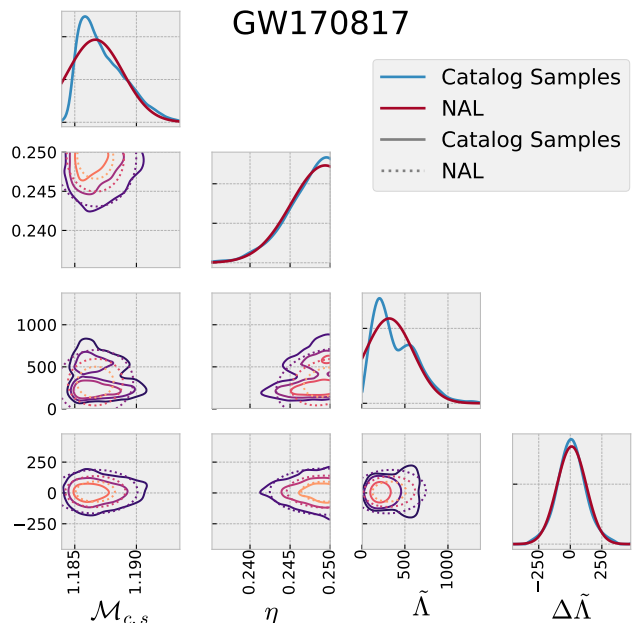


Figure 2. Similar to figure 1. Tidal parameters are fit for BNS mergers. This example includes samples from the IMRPhenomPv2NRT\_lowSpin approximant.

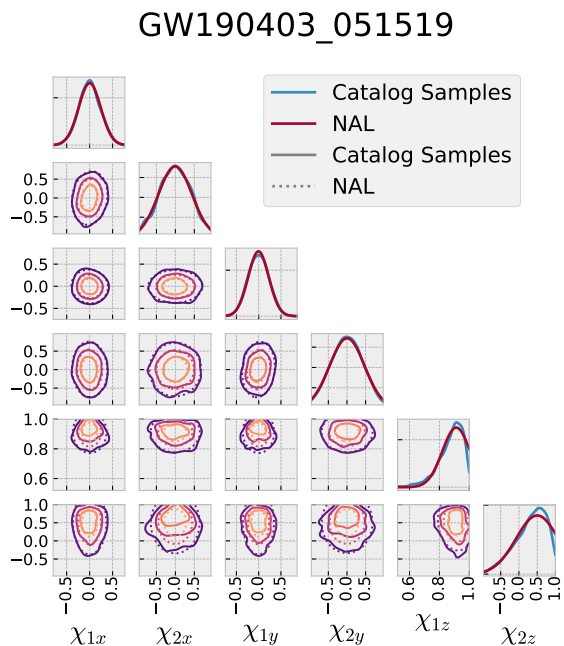


Figure 3. Similar to figure 1. Cartesian spin components are fit, compared with catalog samples. GW190403\_051519 is interesting because of the high degree of certainty for  $\chi_{1z} > 0$ , known to 10 characteristic standard deviations. The SEOBNv4PHM waveform samples for GW190403\_051519 are used for this example.

### III. RESULTS

Figure 4 highlights the agreement between NAL models and the sample distribution for the preferred samples of confident BBH events in O3 for both aligned and precessing spin parameterizations. We find that waveform systematic vastly outweigh the information lost when NAL models are used to represent the sample distribution. The KL divergence-based measure of the quality of each fit is available as part of the associated data release; see Appendix B for details. A bounded multivariate normal distribution in these parameters is sufficient for fully characterizing the astrophysical parameters of events without significant non-Gaussian features (such as bi-modality). This model has many useful properties, including a way to generate random samples, fast likelihood evaluation, symbolic marginalization and transformations, and parameters which describe the Maximum Likelihood Estimate (MLE), uncertainty, and parameter correlation. We provide fits for the mass parameters, distance, aligned spin, tidal deformability, and Cartesian spin components for available samples in the Gravitational-Wave Transient Catalogs [4, 7, 30–32, 34].

Figure 1 shows the advantages of these fits for three-dimensional likelihood approximations, using an aligned spin model. Figure 2 shows the agreement for fits to the tidal parameters  $\tilde{\Lambda}$  and  $\delta\tilde{\Lambda}$  with mass parameters. Tidal parameter fits are available for events/waveform combinations with catalog support, including fits for GW170817 and GW190425. Figure 3 shows an agreement for Cartesian spin components with high spin. Cartesian spin fits are available for event/waveform combinations with catalog support. Examples for different types of fits are provided in table I

#### A. Catalog of models

Figure 5 illustrates some properties of our NAL fits for the GWTC-3 catalog. Specifically, this figure provides point estimates for each event based on our inferred Maximum Likelihood Estimate (MLE) values for  $\mathcal{M}_c$  and  $\eta$  (i.e., it shows our inferred  $\mu$  parameters for each event). Each point estimate is color-coded by a naive frequentist estimate of how similar the mass ratio  $\eta$  is to equal mass, relative to each observation’s individual measurement error.

This figure demonstrates the practical utility of NAL for understanding, communicating, and representing GW parameter information: we can efficiently characterize individual events’ properties and highlight events with notably unique properties, such as unequal masses. For example, in this figure, the six events color-coded in green are manifestly noteworthy as potentially unequal-mass GW sources. The many familiar frequentist diagnostics enabled by NAL should help conceptually identify and differentiate between current and future clusters of observations.

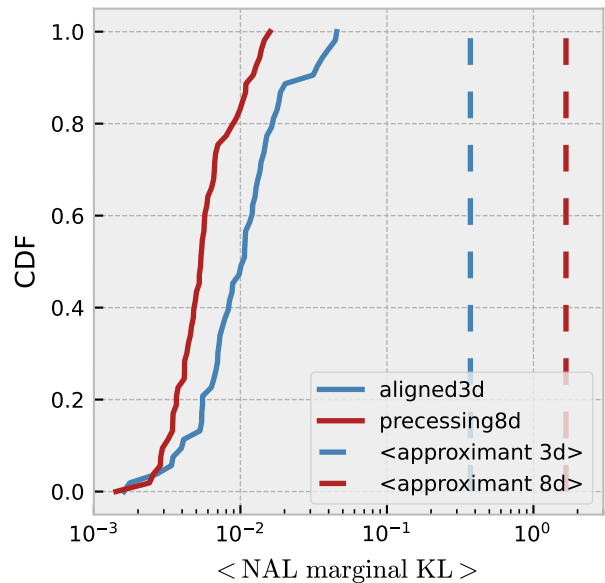


Figure 4. A Cumulative Distribution Function (CDF) for the average of the marginal KL divergences individual events, measuring the agreement between NAL models and the sample distribution. This selection includes the preferred samples for the 53 confident BBH observations in O3, identified by the rates and populations paper [33]. We consider both aligned and precessing spin parameterizations, consistent with table II. The median KL divergence is comparable to or below the most pessimistic scenario ( $1/2N$ ) above which systematics in our likelihood could possibly impact population inference. Vertical lines further characterize the effects of waveform systematics. These lines represent the average analytic KL divergence (Eq:B5) between Gaussians constructed from samples of different waveform approximants (SEOBNRv4PHM and IMRPhenomXPHM for the 22 included events where both are available).

As noted previously, our NAL estimates are distinct from and more accurate than estimates based on the sample mean or median of parameter estimation samples for events with significant effects from a finite boundary in parameter space, such as is seen in the symmetric mass ratio for events with equal mass. As demonstrated by Figure 5, many currently-detectable GW sources are near or consistent with equal mass. Other parameters affected by similar finite boundary effects include spin ( $-1 < \chi_{\text{eff}}, \chi_{i,j} < 1$ ) and neutron star deformability ( $0 < \tilde{\Lambda}$ ), for which an out-of-bounds parameterization is not physical. As the shape of the mass distribution, the spin distribution, and the neutron star equation of state are key questions in this era of gravitational-wave astronomy, better estimates of these parameters are of immediate inherent value to studies of the gravitational-wave population.

We provide NAL fits for many characterizations of the astrophysical parameters for each event in the



Event	Parameters	KL Divergence	KL (simple)
GW190521	$\mathcal{M}_c = 65.6_{-6.5}^{+6.5} M_\odot$ , $\eta = 0.2498_{-0.022}^{+0.0002}$ , $\chi_{\text{eff}} = 0.057_{-0.23}^{+0.23}$	0.016	0.071
GW190408.181802	$\mathcal{M}_{c,z} = 23.53_{-0.94}^{+0.93} M_\odot$ , $\eta = 0.248_{-0.017}^{+0.002}$ , $\chi_{\text{eff}} = -0.04_{-0.10}^{+0.10}$ , $d_L^{-1} = 6.7_{-1.6}^{+1.6} \times 10^{-4} \text{Mpc}^{-1}$	0.033	0.066
GW190425	$\mathcal{M}_c = 1.438_{-0.013}^{+0.013} M_\odot$ , $\eta = 0.227_{-0.018}^{+0.018}$ , $\chi_{\text{eff}} = 0.09_{-0.05}^{+0.05}$ , $\tilde{\Lambda} = 208_{-208}^{+872}$ , $\delta\tilde{\Lambda} = 37_{-37}^{+188}$	0.019	0.037
GW190517.054101	$\mathcal{M}_c = 25.9_{-2.5}^{+2.5} M_\odot$ , $\eta = 0.2498_{-0.023}^{+0.0002}$ , $\chi_{1x} = 0.00_{-0.45}^{+0.45}$ , $\chi_{2x} = 0.00_{-0.48}^{+0.48}$ , $\chi_{1y} = 0.00_{-0.45}^{+0.45}$ , $\chi_{2y} = 0.00_{-0.46}^{+0.46}$ , $\chi_{1z} = 0.66_{-0.19}^{+0.19}$ , $\chi_{2z} = 0.43_{-0.41}^{+0.41}$	0.004	0.019

Table I. Maximum likelihood estimates for choice parameters for a few events, using the “PublicationSamples” samples for GWTC-2. Uncertainties represent the characteristic standard deviation of each fit, adjusted for coordinate boundaries. Included are the KL divergences for the optimized parameterizations, compared with the simple parameterizations inferred from the sample mean and covariance.

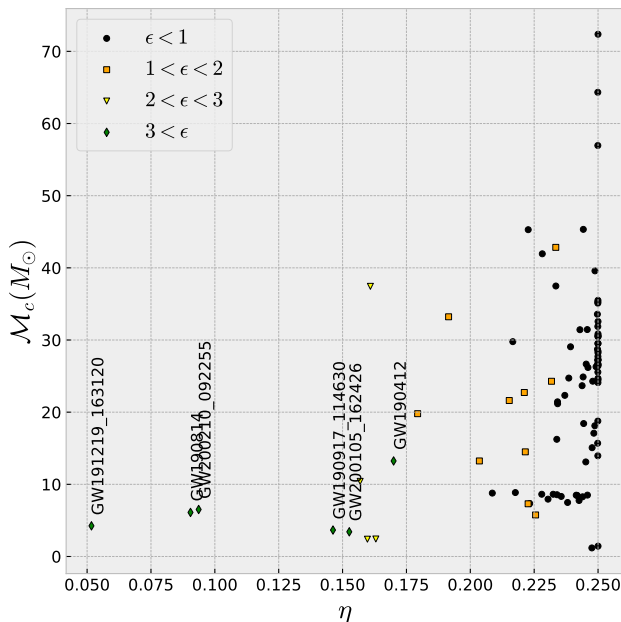


Figure 5. A scatter plot of MLE parameter values for GW events, via aligned3d\_source NAL models, in  $\mathcal{M}_c$  and  $\eta$ . The markers indicated in the legend designate events with statistically significant deviations from equal mass, where  $\epsilon = (1/4 - \mu_\eta)/\sigma_\eta$ .

Gravitational-wave Transient Catalogs, for every available waveform approximant in the posterior samples released. We provide fits for Cartesian spin components and tidal deformability parameters for waveform approximants that support those parameters. Table II (in appendix C) outlines the types of fits available in our data products, as well as the prior removed from each associated set of samples.

## IV. APPLICATIONS

While providing a compact, interpretable representation of GW inferences provides the primary justification for using an NAL representation, our approach also opens up additional opportunities. The following sections briefly summarize two opportunities in low-latency parameter inference and in population inference, respectively; see

### A. Opportunities for low latency parameter estimation

In the coming observing runs for ground-based gravitational-wave detectors, there is a need for low-latency parameterization for the potential follow-up of electromagnetic counter-parts to gravitational-wave observations. Many groups are working to address this challenge, using a variety of methods [1, 29, 39, 48, 50, 78, 98] Our Gaussian approximations can be efficiently built from sparse training data. We can train these Gaussians using either posterior samples or marginal likelihoods, such as the outputs of the RIFT parameter inference engine. As a result, NAL can be an ingredient in or an outcome of low-latency parameter inference. NAL parameterizations also offer an opportunity to interpret posterior sample outputs from other low-latency approaches such as the output of a neural net (for example, [39]).

As a concrete example, Figure 6 shows the results of reconstructing GW190412 with IMRPhenomD, based on marginal likelihoods for (detector-frame) masses and spins provided by RIFT on an initial, weakly-targeted set of candidate evaluation points in the neighborhood of the binary parameters flagged by a search for follow-up. In this proof-of-concept we employ the detector-frame masses without significant loss of generality, because most binary sources meriting follow-up will occur at low redshift and therefore have minimal practical difference between their detector and source frame masses. In this example, a set of points in  $(\mathcal{M}_c, \eta, \chi_{\text{eff}})_k$  are

## GW190412

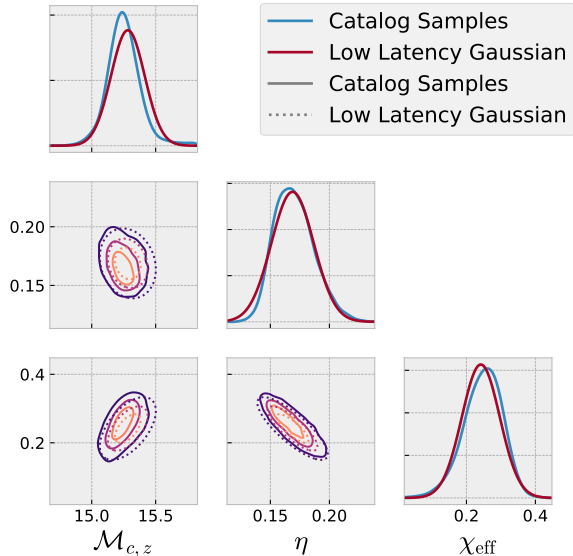


Figure 6. Analysis of GW190412 with NAL based on a limited likelihood inputs from RIFT designed to mimic a “low-latency” analysis, using IMRPhenomD. For comparison, we also show the inferred marginal likelihood derived from the discovery publication for GW190412, as provided in GWTC-2 as “PublicationSamples”. Even though the NAL approximation was derived with a different waveform, different physics (no precession), and various different analysis settings than the production results, we find reasonable agreement between this low-latency approach and longer-timescale investigations.

evaluated with RIFT to produce a marginal likelihood  $\mathcal{L}$ , which we in turn approximate using NAL. Including queuing and startup time, the marginal likelihoods can be evaluated within a few seconds, followed by a comparable timescale for the associated Gaussian approximation and posterior.

The NAL result closely conforms to the results of an extended RIFT analysis with comparable settings. While imperfectly capturing the full range of parameters allowed by more comprehensive physics and waveform systematics, this fast approximation could be one fruitful method to quickly characterize binary sources, particularly for downstream rapid population analysis.

We defer a systematic demonstration of and validation study for NAL for low-latency PE to a dedicated publication.

## B. Population inference

NAL models can also be efficiently used within population inference calculations, to evaluate the necessary event-marginal likelihoods  $\int dx \mathcal{L}_n(x) p(x|\Lambda)$  that arise when assessing how well a set of individual event likelihoods  $\mathcal{L}_n(x)$  match the predictions of a parameterized

population  $p(x|\Lambda)$ , where  $x$  are binary parameters and  $\Lambda$  are population parameters. The NAL approach provides a fast likelihood and even natural Monte Carlo sampling method for  $\mathcal{L}_n$ , enabling us to efficiently evaluate each of these integrals.

The NAL method is particularly powerful when  $p(x|\Lambda)$  is a generative model only available via Monte Carlo. Many astrophysical models are formulated by such Monte Carlo techniques, notably including isolated binary evolution but also many scenarios for dynamical formation [12, 19, 23, 33, 46, 96, 100, 106, 109, 116]. In our previous work we have demonstrated how to use these Gaussian approximations efficiently with these generative models [41, 45]. For some applications, a direct evaluation of the likelihood is desired, such as constraining the neutron star equation of state [42, 54, 55, 95, 117].

The fast likelihood evaluations afforded by NAL compare favorably to the speed and accuracy provided by other methods particularly in high dimensions. For instance, a kernel density estimate constructed using the fair draws from a posterior or likelihood will be slower by a factor that goes as the number of samples used to construct the estimate (as each sample is represented by a Gaussian for a standard KDE). This is worsened by the requirement of more and more samples for a kernel density estimate as the dimensionality of the space explored increases. When only a fixed number of samples are available, there is a limit to the number of dimensions that can be explored without losing accuracy.

To illustrate how NAL facilitate efficient comparisons of large population synthesis models to observations, Figure 7, drawn from VD’s Ph.D. dissertation [40], shows the likelihood comparison for a one-dimensional binary evolution study, focusing on the characteristic value for the Maxwellian black-hole kick velocity assumed by the binary evolution model. The M15 synthetic universe (the preferred model with the highest likelihood) is based on the M13 simulation from Belczynski et al. (2020)[19], with the only difference being the characteristic value of the Maxwellian black hole kick velocity, which takes a value of 130km/s. This likelihood estimation requires an evaluation of the likelihood describing the agreement of each simulated binary (for example, M15 consists of 26 million such binaries) to each gravitational-wave observation A kernel density estimate (considering the full set of samples) for this event would require an evaluation of 26 million Gaussians for each point where you want to evaluate the likelihood, while a NAL model requires only one. This quantifies the speed advantage that NAL models have over kernel density estimates in particular, and we argue that more complicated methods of evaluating an approximate likelihood will not generally be faster than a single Gaussian evaluation. This particular example (figure 7) demonstrates this use-case for NAL models.

As the number of events observed by gravitational-wave observatories increases, the computational cost of these likelihood evaluations becomes increasingly impor-



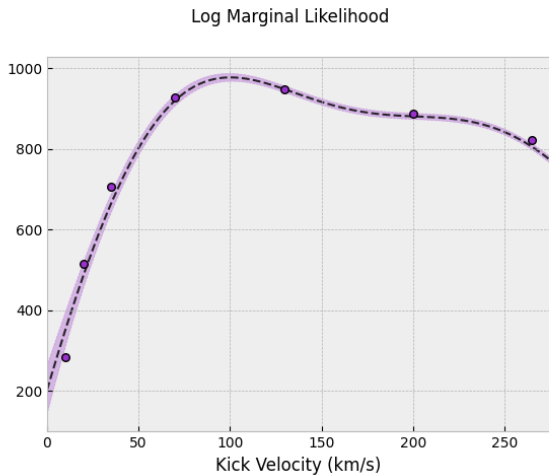


Figure 7. Illustration of the utility of NAL: This population synthesis example explores the agreement of binary evolution simulations to the observed confident detections in the first part of LIGO’s third observing run. The likelihood for each simulation is evaluated using NAL models to consider the agreement of each simulated binary to each gravitational-wave observation. This figure originally appeared in previous work [40].

tant. NAL models will readily meet this challenge, as a single Gaussian evaluation for each event will cost less than a kernel density estimate for a single event, even if the number of events approaches the thousands. An in-depth discussion of the binary evolution model and hierarchical inference involved in this example are beyond the scope of this paper, but are readily available in the dissertation [40].

## V. CONCLUSIONS

In this paper, we demonstrate that using NAL models, we can take full advantage of the properties of the multivariate normal distribution without introducing a bias through finite boundary effects. We demonstrate further that these models succeed in reconstructing high dimensional likelihood functions for the parameter estimation samples with Cartesian spin components and tidal parameters. These likelihood models provide the full advantages of the properties of the multivariate normal distribution (fast evaluation, sampling methods, and symbolic transformations). Furthermore, the  $\mu$  parameters of each significantly truncated Gaussian directly identify the location of maximum likelihood estimate more accurately than the sample mean or median. Therefore, NAL fits provide an advantage for population studies wherever the sample mean or median would be employed as the single parameter estimate for a gravitational-wave event.

Many other groups estimate the marginal likelihood function for each event directly from posterior samples [2, 28, 42, 54, 55, 67, 74]. While these methods have

a high degree of accuracy, they suffer from computational limitations, especially for higher dimensional parameter spaces. Leading into O4, population studies will be forced to move away from using entire catalogs of samples to characterize the likelihood for each gravitational-wave event as the sensitivity of the detector increases and detections become more abundant [52]. This simple parametric approximation to that likelihood function provides a reliable tool which will continue to perform well as the scale of analysis increases, and already perform well to reconstruct the full astrophysical parameter space for gravitational-wave events in a computationally efficient way.

At the time of submission of this publication, we make the NAL models available publicly at <https://gitlab.com/xevra/nal-data>, as well as the code repository used to make these fits, Gravitational-Wave Approximate Likelihood (GWALK) at <https://gitlab.com/xevra/gwalk>. An intermediate step in the construction of NAL models involves using a Gaussian Process Regression algorithm to model parameter estimation samples [111]. Our Gaussian Process code is available at <https://gitlab.com/xevra/gaussian-process-api>.

## ACKNOWLEDGMENTS

The authors thank Patricia Schmidt for helpful feedback. ROS, VD, and AY are supported by NSF-PHY 2012057; ROS is also supported via NSF PHY-1912632 and AST-1909534. VD is supported by an appointment to the NASA Postdoctoral Program at the NASA Goddard Space Flight Center administered by Oak Ridge Associated Universities under contract NPP-GSFC-NOV21-0031. DW thanks the NSF (PHY-1912649) for support. This material is based upon work supported by NSF’s LIGO Laboratory which is a major facility fully funded by the National Science Foundation. This research has made use of data, software and/or web tools obtained from the Gravitational Wave Open Science Center (<https://www.gw-openscience.org/>), a service of LIGO Laboratory, the LIGO Scientific Collaboration and the Virgo Collaboration. LIGO Laboratory and Advanced LIGO are funded by the United States National Science Foundation (NSF) as well as the Science and Technology Facilities Council (STFC) of the United Kingdom, the Max-Planck-Society (MPS), and the State of Niedersachsen/Germany for support of the construction of Advanced LIGO and construction and operation of the GEO600 detector. Additional support for Advanced LIGO was provided by the Australian Research Council. Virgo is funded through the European Gravitational Observatory (EGO), by the French Centre National de Recherche Scientifique (CNRS), the Italian Istituto Nazionale di Fisica Nucleare (INFN), and the Dutch Nikhef, with contributions by institutions from Belgium, Germany, Greece, Hungary, Ireland, Japan, Monaco, Poland, Portugal, Spain. The authors are grate-

ful for computational resources provided by the LIGO Laboratory and supported by National Science Foundation Grants PHY-0757058 and PHY-0823459. We acknowledge software packages used in producing the gaussian-process-api and GWALK software associated with this publication and the associated data release, including NUMPY [57], SCIPY [110], MATPLOTLIB [63], CYTHON [18], ASTROPY [14, 15], and H5PY [35].

### Appendix A: Impact of systematics on population inferences

In the introduction, we outlined how systematic errors in our likelihood estimate propagate into population results. In this appendix, we provide a more generic treatment. Our approach applies to *any* systematic, be it deterministic or stochastic, notably including inaccuracy in the likelihood estimate (e.g., due to a Gaussian or other approximation; due to limited sample size) and including waveform systematics. Since stochastic systematics largely average out, our discussion will emphasize the impact of deterministic effects. In the discussion below, our notation will follow Appendix C in [116].

We consider a systematic controlled by one deterministic parameter  $s$ . This parameter could control interpolation between an exact and a gaussian approximation; waveform systematics; or some other measure of smallness. Each single-event likelihood realization  $\mathcal{L}(x|s)$  can be expanded in a series in  $s$ . For the purposes of this discussion we'll only retain terms to linear order:

$$\mathcal{L}(x|s) \simeq \mathcal{L}(x|0) + s\partial_s\mathcal{L} + \dots$$

For simplicity omitting selection effects, the population likelihood  $L_{\text{pop}}$  is the product of single-event likelihoods

$$L_{\text{pop}} = \prod_k \mathcal{L}_k(x|s) \simeq \left[ \prod_k \mathcal{L}_k(x|0) \right] \left( 1 + s \sum_k \frac{\partial_s \mathcal{L}_k}{\mathcal{L}_k} \right) \quad (\text{A1})$$

To assess the impact of systematics in the limit of many observations, we consider the *population-averaged log-likelihood*, relative to a population  $p(x|\Lambda)$ :

$$\begin{aligned} \langle \ln L_{\text{pop}} \rangle_{\text{pop}} &\equiv N \int p(x|\Lambda) \ln \mathcal{L}(x|s) \\ &\simeq \ln L_{\text{pop}}(0|\Lambda) + sN \int p(x|\Lambda) \partial_s \ln \mathcal{L}(x|s)_{s=0} \end{aligned} \quad (\text{A2})$$

The first term characterizes the likelihood in the absence of systematics. In the limit of many observations, we assume this expression has a single global maximum, without loss of generality at the origin  $\Lambda \simeq 0$ . Expanding the first term to quadratic order in  $\Lambda$  and the second term

to linear order as

$$\ln L_{\text{pop}}(0|\Lambda) \simeq \text{const} - \frac{1}{2} N \hat{\Gamma}_{ab} \Lambda_a \Lambda_b \quad (\text{A3})$$

$$G \equiv \int p(x|\Lambda) \partial_s \ln \mathcal{L}(x|s)_{s=0} \simeq \text{const} + \Lambda_a \partial_a G \quad (\text{A4})$$

we can show the population-averaged log likelihood has a global maximum of the form

$$\langle \ln L_{\text{pop}} \rangle_{\text{pop}} = \text{const} - \frac{1}{2} N \Gamma_{ab} (\Lambda - \Lambda_0)_a (\Lambda - \Lambda_0)_b \quad (\text{A5})$$

$$\Lambda_{0,a} = s \hat{\Sigma}_{ab} \partial_b G \quad (\text{A6})$$

where  $\hat{\Sigma} = \hat{\Gamma}^{-1}$ . This final expression for  $\Lambda_0$  expresses population hyperparameter biases in terms of (derivatives of)  $G$ , where  $G$  represents population-averaged measurement errors. In short, we can *calculate* the expected impact of systematics on population hyperparameter inferences.

While exact results for realistic systematics like waveform uncertainty are computationally inaccessible or stochastic, we can capture the essential features of many systematic errors with simple toy models. Calculations of this form will reproduce the simple order-of-magnitude estimates described in the introduction.

### Appendix B: Optimization and Goodness of Fit for Non-parametric and Parametric Models

#### 1. Non-parametric Likelihood Interpolation

In this section, we describe how the Gaussian processes which describe the one- and two-dimensional marginal distributions are trained, and how error is systematically minimized at each step. Let  $\mathbf{x}$  refer to a one or two dimensional set of parameter space. We begin by using one- and two-dimensional histograms to model the density of the catalog samples. For some number of bins,  $n$ , a histogram is constructed, representing the posterior samples as a likelihood by weighing each sample by the inverse prior. In this section, we call the centers of each bin  $X_n$ , and the bin values, normalized as a density,  $Y_n$ . A Gaussian Process (GP),  $f_n(\mathbf{x})$ , is trained using  $X_n$  and  $Y_n$ , with training error estimated from weighted histogram bins through the use of binomial fraction estimation:

$$\sigma_{\text{hist}} = \sqrt{p \times (1 - p)} \quad (\text{B1})$$

These Gaussian processes make use of sparse Cholesky decomposition and cython compiled basis functions [111]. We provide this GP as a library at <https://gitlab.com/xevra/gaussian-process-api>.

We then construct a similar histogram with  $n+1$  bins, along with a similar GP,  $f_{n+1}(\mathbf{x})$ , trained using  $X_{n+1}$  and  $Y_{n+1}$ . We then cross-evaluate  $f_n$  and  $f_{n+1}$  on each respective training set.

$$\delta Y_n = |Y_n - f_{n+1}(X_n)| \quad (\text{B2})$$

$$\delta Y_{n+1} = |Y_{n+1} - f_n(X_{n+1})| \quad (\text{B3})$$

We call this the "residual error", and We find that by minimizing these errors, using the Kolmogorov-Smirnov test [71], we select an optimal number of bins for our histogram. Once this optimization is complete, we train another GP using both sets of training data (for  $n$  and  $n + 1$ ). For this final model, training error is estimated using the sum in quadrature of histogram error and the residual error. This final GP for each marginalization,  $f(\mathbf{x})$ , will therefore have finer resolution than either  $f_n(\mathbf{x})$  or  $f_{n+1}(\mathbf{x})$ .

## 2. NAL Optimization and Error Handling

The goodness of fit criterion for the NAL models are evaluated using a discretized Kullback-Leibler (KL) divergence, comparing the NAL approximation of  $\mathcal{L}(\mathbf{x})$  to that of the Gaussian process for each marginalization, ( $f(\mathbf{x})$ ) [72]. The KL divergence describes the amount of information lost by us a distribution Q to describe a reference distribution, P. The KL divergence of a discrete random variable  $x$ , from a space  $\mathcal{X}$ , is given by:

$$\text{KL}(P|Q) = \sum_{x \in \mathcal{X}} p(x) \cdot \log \frac{p(x)}{q(x)} \quad (\text{B4})$$

For two multivariate normal distributions, the KL divergence is known analytically:

$$\text{KL}(P|Q) = \frac{1}{2} [(\mu_2 - \mu_1)^T \Sigma_2^{-1} (\mu_2 - \mu_1) + \quad (\text{B5})$$

$$\text{tr}(\Sigma_2^{-1} \Sigma_1) - \ln \frac{|\Sigma_1|}{|\Sigma_2|} - n] \quad (\text{B6})$$

A two dimensional multivariate normal distribution offset in  $\mu$  by one  $\sigma$  in one dimension will therefore have a KL divergence of 0.5.

The evaluation of the KL divergence on each NAL model is carried out using a grid of 100 points in each dimension inside our bounded region (100 points for 1D marginalizations and 10,000 points for 2D marginalizations). We use a maximum likelihood estimate approach in optimizing the fit parameters for our higher-dimensional Gaussians, taking advantage of the one- and two-dimensional kl divergence information available. The mean of the one- and two dimensional kl divergences is used to describe the goodness of fit for each bounded multivariate-normal distribution included in the associated data release.

## Appendix C: GWALK Parameterizations

- 
- [1] J. Aasi, J. Abadie, B. P. Abbott, R. Abbott, and et al. FIRST SEARCHES FOR OPTICAL COUNTERPARTS TO GRAVITATIONAL-WAVE CANDIDATE EVENTS. *The Astrophysical Journal Supplement Series*, 211(1):7, feb 2014.
  - [2] B. Abbott, R. Abbott, T. Abbott, M. Abernathy, and et al. Directly comparing gw150914 with numerical solutions of einstein's equations for binary black hole coalescence. *Physical Review D*, 94(6), Sep 2016.
  - [3] B. Abbott, R. Abbott, T. Abbott, M. Abernathy, and et al. Gw150914: First results from the search for binary black hole coalescence with advanced ligo. *Physical Review D*, 93(12), Jun 2016.
  - [4] B. Abbott, R. Abbott, T. Abbott, S. Abraham, and et al. Gwtc-1: a gravitational-wave transient catalog of compact binary mergers observed by ligo and virgo during the first and second observing runs. *Physical Review X*, 9(3):031040, 2019.
  - [5] B. P. Abbott, R. Abbott, T. D. Abbott, S. Abraham, and et al. Binary black hole population properties inferred from the first and second observing runs of advanced ligo and advanced virgo. *The Astrophysical Journal*, 882(2):L24, Sep 2019.
  - [6] B. P. Abbott, R. Abbott, T. D. Abbott, S. Abraham, and et al. Prospects for observing and localizing gravitational-wave transients with advanced LIGO, advanced virgo and KAGRA. *Living Reviews in Relativity*, 23(1), sep 2020.
  - [7] R. Abbott, T. Abbott, S. Abraham, F. Acernese, and et al. Gwtc-2: Compact binary coalescences observed by ligo and virgo during the first half of the third observing run. *Physical Review X*, 11(2):021053, 2021.
  - [8] B. Abbott et al. (The LIGO Scientific Collaboration and the Virgo Collaboration). Astrophysical Implications of the Binary Black-hole Merger GW150914. *Astrophysical Journal*, 818:L22, Feb. 2016.
  - [9] F. Acernese, M. Agathos, K. Agatsuma, D. Aisa, and et al. Advanced virgo: a second-generation interferometric gravitational wave detector. *Classical and Quantum Gravity*, 32(2):024001, dec 2014.
  - [10] S. Akcay, S. Bernuzzi, F. Messina, A. Nagar, N. Ortiz, and P. Rettengo. Effective-one-body multipolar waveform for tidally interacting binary neutron stars up to merger. *Phys. Rev. D*, 99(4):044051, 2019.
  - [11] M. Al-Mamun, A. W. Steiner, J. Nättilä, J. Lange, R. O'Shaughnessy, I. Tews, S. Gandolfi, C. Heinke, and S. Han. Combining Electromagnetic and Gravitational-Wave Constraints on Neutron-Star Masses and Radii. *Phys. Rev. Lett*, 126(6):061101, Feb. 2021.
  - [12] G. Ashton, M. Hübner, P. D. Lasky, C. Talbot, K. Ackley, S. Biscoveanu, Q. Chu, A. Divakarla, P. J. Easter, B. Goncharov, F. H. Vivanco, J. Harms, M. E. Lower,

Parameterization	Coordinates	Prior
aligned3d	$\mathcal{M}_{c,z}, \eta, \chi_{\text{eff}}$	aligned3d
aligned3d_source	$\mathcal{M}_c, \eta, \chi_{\text{eff}}$	aligned3d
aligned3d_dist	$\mathcal{M}_{c,z}, \eta, \chi_{\text{eff}}, d_L^{-1}$	aligned3d_dist
mass_tides	$\mathcal{M}_{c,z}, \eta, \tilde{\Lambda}, \delta\tilde{\Lambda}$	mass
mass_tides_source	$\mathcal{M}_c, \eta, \tilde{\Lambda}, \delta\tilde{\Lambda}$	mass
aligned_tides	$\mathcal{M}_{c,z}, \eta, \chi_{\text{eff}}, \tilde{\Lambda}, \delta\tilde{\Lambda}$	aligned3d
aligned_tides_source	$\mathcal{M}_c, \eta, \chi_{\text{eff}}, \tilde{\Lambda}, \delta\tilde{\Lambda}$	aligned3d
aligned_tides_dist	$\mathcal{M}_{c,z}, \eta, \chi_{\text{eff}}, \tilde{\Lambda}, \delta\tilde{\Lambda}, d_L^{-1}$	aligned3d_dist
spin6d	$\chi_{1x}, \chi_{2x}, \chi_{1y}, \chi_{2y}, \chi_{1z}, \chi_{2z}$	precessing8d
precessing8d	$\mathcal{M}_{c,z}, \eta, \chi_{1x}, \chi_{2x}, \chi_{1y}, \chi_{2y}, \chi_{1z}, \chi_{2z}$	precessing8d
precessing8d_source	$\mathcal{M}_c, \eta, \chi_{1x}, \chi_{2x}, \chi_{1y}, \chi_{2y}, \chi_{1z}, \chi_{2z}$	precessing8d
precessing8d_dist	$\mathcal{M}_{c,z}, \eta, \chi_{1x}, \chi_{2x}, \chi_{1y}, \chi_{2y}, \chi_{1z}, \chi_{2z}, d_L^{-1}$	precessing8d_dist
precessing_tides_source	$\mathcal{M}_c, \eta, \chi_{1x}, \chi_{2x}, \chi_{1y}, \chi_{2y}, \chi_{1z}, \chi_{2z}, \tilde{\Lambda}, \delta\tilde{\Lambda}$	precessing8d
full_precessing_tides	$\mathcal{M}_{c,z}, \eta, \chi_{1x}, \chi_{2x}, \chi_{1y}, \chi_{2y}, \chi_{1z}, \chi_{2z}, \tilde{\Lambda}, \delta\tilde{\Lambda}, d_L^{-1}$	precessing8d_dist

Table II. Here, we define the parameterization labels used in our study, and the associated code/data releases.

In table II, we describe the labels used in the data release to keep track of the parameters included in each type of model. We further clarify that  $\mathcal{M}_{c,z}$  is a detector-frame chirp mass,  $\mathcal{M}_c$  is a source-frame chirp mass,  $\eta$  is the symmetric mass ratio,  $d_L^{-1}$  is the inverse of the luminosity distance,  $\tilde{\Lambda}$  and  $\delta\tilde{\Lambda}$  are the tidal parameters,  $\chi_{\text{eff}}$  is the aligned spin in the plane of the orbit, and  $\chi_{ij}$  is the spin of the  $i$ -th object (1 or 2) in the  $j$  dimension (x, y, or z). The labeling of the prior which is removed from the posterior samples for each fit corresponds to the simplest parameterization label which removes the same prior. All models must account for the mass prior, and some must account for distance. The uninformative spin prior is removed for different spin parameterizations (see sec II A).

- G. D. Meadors, D. Melchor, E. Payne, M. D. Pitkin, J. Powell, N. Sarin, R. J. E. Smith, and E. Thrane. Bilby: A user-friendly bayesian inference library for gravitational-wave astronomy. *The Astrophysical Journal Supplement Series*, 241(2):27, apr 2019.
- [13] Y. Aso, Y. Michimura, K. Somiya, M. Ando, and et al. Interferometer design of the kagra gravitational wave detector. *Phys. Rev. D*, 88:043007, Aug 2013.
- [14] Astropy Collaboration, A. M. Price-Whelan, B. M. Sipőcz, H. M. Günther, and et al. The Astropy Project: Building an Open-science Project and Status of the v2.0 Core Package. *Astronomical Journal*, 156(3):123, Sept. 2018.
- [15] Astropy Collaboration, T. P. Robitaille, E. J. Tollerud, P. Greenfield, and et al. Astropy: A community Python package for astronomy. *A&A*, 558:A33, Oct. 2013.
- [16] B. Aylott, J. G. Baker, W. D. Boggs, and M. B. et al. Testing gravitational-wave searches with numerical relativity waveforms: results from the first numerical INJECTION analysis (NINJA) project. *Classical and Quantum Gravity*, 26(16):165008, aug 2009.
- [17] T. Bayes. An essay towards solving a problem in the doctrine of chances. *Phil. Trans. of the Royal Soc. of London*, 53:370–418, 1763.
- [18] S. Behnel, R. Bradshaw, C. Citro, L. Dalcin, D. S. Seljebotn, and K. Smith. Cython: The best of both worlds. *Computing in Science & Engineering*, 13(2):31–39, 2011.
- [19] K. Belczynski, J. Klencki, C. E. Fields, A. Olejak, and et al. Evolutionary roads leading to low effective spins, high black hole masses, and o1/o2 rates for ligo/virgo binary black holes. *Astronomy & Astrophysics*, 636:A104, Apr 2020.
- [20] C. M. Biwer, C. D. Capano, S. De, M. Cabero, and et al. PyCBC Inference: A Python-based Parameter Estimation Toolkit for Compact Binary Coalescence Signal. *PASP*, 131(996):024503, Feb. 2019.
- [21] A. Bohé et al. Improved effective-one-body model of spinning, nonprecessing binary black holes for the era of gravitational-wave astrophysics with advanced detectors. *Phys. Rev. D*, 95(4):044028, 2017.
- [22] M. Boyle, D. Hemberger, D. A. B. Iozzo, G. Lovelace, and et al. The SXS collaboration catalog of binary black hole simulations. *Classical and Quantum Gravity*, 36(19):195006, sep 2019.
- [23] K. Breivik, S. Coughlin, M. Zevin, C. L. Rodriguez, K. Kremer, C. S. Ye, J. J. Andrews, M. Kurkowski, M. C. Digman, S. L. Larson, and F. A. Rasio. COSMIC variance in binary population synthesis. *The Astrophysical Journal*, 898(1):71, jul 2020.
- [24] F. S. Broekgaarden and E. Berger. Formation of the first two black hole–neutron star mergers (gw200115 and gw200105) from isolated binary evolution. *The Astrophysical Journal Letters*, 920(1):L13, 2021.
- [25] B. Brügmann, J. A. González, M. Hannam, S. Husa, U. Sperhake, and W. Tichy. Calibration of moving puncture simulations. *Physical Review D*, 77(2), jan 2008.
- [26] T. A. Callister. A Thesaurus for Common Priors in Gravitational-Wave Astronomy. *arXiv e-prints*, page arXiv:2104.09508, Apr. 2021.
- [27] H. Cho, E. Ochsner, R. O’Shaughnessy, C. Kim, and C. Lee. Gravitational waves from BH-NS binaries: Phenomenological Fisher matrices and parameter estimation using higher harmonics. *Phys. Rev. D*, 87:02400–+, Jan. 2013.
- [28] H.-S. Cho, E. Ochsner, R. O’Shaughnessy, C. Kim, and C.-H. Lee. Gravitational waves from black hole-neutron star binaries: Effective fisher matrices and parameter

- estimation using higher harmonics. *Physical Review D*, 87(2), Jan 2013.
- [29] L. S. Collaboration and V. Collaboration. Ligo/virgo public alerts user guide. 2019.
- [30] L. S. Collaboration and V. Collaboration. GWTC-2.1: Deep Extended Catalog of Compact Binary Coalescences Observed by LIGO and Virgo During the First Half of the Third Observing Run - Parameter Estimation Data Release, July 2021.
- [31] L. S. Collaboration, V. Collaboration, and K. Collaboration. GWTC-3: Compact Binary Coalescences Observed by LIGO and Virgo During the Second Part of the Third Observing Run — Parameter estimation data release, Nov. 2021.
- [32] T. L. S. Collaboration, the Virgo Collaboration, and the KAGRA Collaboration et al. Gwtc-3: Compact binary coalescences observed by ligo and virgo during the second part of the third observing run, 2021.
- [33] T. L. S. Collaboration, the Virgo Collaboration, and the KAGRA Collaboration et al. The population of merging compact binaries inferred using gravitational waves through gwtc-3, 2021.
- [34] T. L. S. Collaboration and the Virgo Collaboration et al. Gwtc-2.1: Deep extended catalog of compact binary coalescences observed by ligo and virgo during the first half of the third observing run, 2021.
- [35] A. Collette. *Python and HDF5*. O’Reilly, 2013.
- [36] N. J. Cornish. Fast fisher matrices and lazy likelihoods, 2010.
- [37] N. J. Cornish. Heterodyned likelihood for rapid gravitational wave parameter inference. *Physical Review D*, 104(10), nov 2021.
- [38] R. Cotesta, A. Buonanno, A. Bohé, A. Taracchini, I. Hinder, and S. Ossokine. Enriching the Symphony of Gravitational Waves from Binary Black Holes by Tuning Higher Harmonics. *Phys. Rev. D*, 98(8):084028, 2018.
- [39] M. Dax, S. R. Green, J. Gair, J. H. Macke, A. Buonanno, and B. Schölkopf. Real-time gravitational wave science with neural posterior estimation. *Phys. Rev. Lett.*, 127:241103, Dec 2021.
- [40] V. Del Favero. Constraints on compact binary formation and effective gravitational wave likelihood approximation. 2022.
- [41] V. Delfavero, R. O’Shaughnessy, D. Wysocki, and A. Yellikar. Normal approximate likelihoods to gravitational wave events. 2021.
- [42] V. D’Emilio, R. Green, and V. Raymond. Density estimation with gaussian processes for gravitational wave posteriors. *Monthly Notices of the Royal Astronomical Society*, 508(2):2090–2097, sep 2021.
- [43] T. Dietrich, S. Bernuzzi, and W. Tichy. Closed-form tidal approximants for binary neutron star gravitational waveforms constructed from high-resolution numerical relativity simulations. *Phys. Rev. D*, 96(12):121501, 2017.
- [44] T. Dietrich, A. Samajdar, S. Khan, N. K. Johnson-McDaniel, R. Dudi, and W. Tichy. Improving the NR-Tidal model for binary neutron star systems. *Phys. Rev. D*, 100(4):044003, 2019.
- [45] Z. Doctor, D. Wysocki, R. O’Shaughnessy, D. E. Holz, and B. Farr. Black Hole Coagulation: Modeling Hierarchical Mergers in Black Hole Populations. *Astrophysical Journal*, 893(1):35, Apr. 2020.
- [46] B. Edelman, F. J. Rivera-Paleo, J. D. Merritt, B. Farr, and et al. Constraining unmodeled physics with compact binary mergers from gwtc-1. *Phys. Rev. D*, 103:042004, Feb 2021.
- [47] R. Essick and W. Farr. Precision Requirements for Monte Carlo Sums within Hierarchical Bayesian Inference. *arXiv e-prints*, page arXiv:2204.00461, Apr. 2022.
- [48] P. A. Evans, J. K. Fridriksson, N. Gehrels, J. Homan, and et al. SWIFT FOLLOW-UP OBSERVATIONS OF CANDIDATE GRAVITATIONAL-WAVE TRANSIENT EVENTS. *The Astrophysical Journal Supplement Series*, 203(2):28, nov 2012.
- [49] W. M. Farr. Accuracy Requirements for Empirically Measured Selection Functions. *Research Notes of the American Astronomical Society*, 3(5):66, May 2019.
- [50] D. Finstad and D. A. Brown. Fast parameter estimation of binary mergers for multimessenger follow-up. *The Astrophysical Journal*, 905(1):L9, dec 2020.
- [51] T. Fragos, J. J. Andrews, S. S. Bavera, C. P. L. Berry, S. Coughlin, A. Dotter, P. Giri, V. Kalogera, A. Katsaggelos, K. Kovlakas, S. Lalvani, D. Misra, P. M. Srivastava, Y. Qin, K. A. Rocha, J. Roman-Garza, J. G. Serra, P. Stahle, M. Sun, X. Teng, G. Trajcevski, N. H. Tran, Z. Xing, E. Zapartas, and M. Zevin. Posydon: A general-purpose population synthesis code with detailed binary-evolution simulations, 2022.
- [52] P. Fritschel, L. S. Collaboration, et al. Instrument science white paper 2020. *Technical Report LIGO-T2000407-v3*, 2020.
- [53] C. García-Quirós, M. Colleoni, S. Husa, H. Estellés, G. Pratten, A. Ramos-Buades, M. Mateu-Lucena, and R. Jaume. Multimode frequency-domain model for the gravitational wave signal from nonprecessing black-hole binaries. *Phys. Rev. D*, 102(6):064002, 2020.
- [54] S. Ghosh, X. Liu, J. Creighton, I. M. n. Hernandez, W. Kastaun, and G. Pratten. Rapid model comparison of equations of state from gravitational wave observation of binary neutron star coalescences. *Phys. Rev. D*, 104:083003, Oct 2021.
- [55] J. Golomb and C. Talbot. Hierarchical inference of binary neutron star mass distribution and equation of state with gravitational waves. *The Astrophysical Journal*, 926(1):79, feb 2022.
- [56] M. Hannam, P. Schmidt, A. Bohé, L. Haegel, S. Husa, F. Ohme, G. Pratten, and M. Pürrer. Simple Model of Complete Precessing Black-Hole-Binary Gravitational Waveforms. *Phys. Rev. Lett.*, 113(15):151101, 2014.
- [57] C. R. Harris, K. J. Millman, S. J. van der Walt, R. Gommers, and et al. Array programming with NumPy. *Nature*, 585(7825):357–362, Sept. 2020.
- [58] J. Healy, C. O. Lousto, J. Lange, and R. O’Shaughnessy. Application of the third RIT binary black hole simulations catalog to parameter estimation of gravitational-wave signals from the LIGO-Virgo O1 and O2 observational runs. *Phys. Rev. D*, 102(12):124053, Dec. 2020.
- [59] F. Hernandez Vivanco, R. Smith, E. Thrane, and P. D. Lasky. A scalable random forest regressor for combining neutron-star equation of state measurements: a case study with GW170817 and GW190425. *MNRAS*, 499(4):5972–5977, Dec. 2020.
- [60] I. Hinder, A. Buonanno, M. Boyle, and Z. B. E. et al. Error-analysis and comparison to analytical models of numerical waveforms produced by the NRAR collaboration. *Classical and Quantum Gravity*, 31(2):025012,

- jan 2013.
- [61] T. Hinderer et al. Effects of neutron-star dynamic tides on gravitational waveforms within the effective-one-body approach. *Phys. Rev. Lett.*, 116(18):181101, 2016.
- [62] Y. Huang, C.-J. Haster, J. Roulet, S. Vitale, and et al. Source properties of the lowest signal-to-noise-ratio binary black hole detections. *Phys. Rev. D*, 102(10):103024, Nov. 2020.
- [63] J. D. Hunter. Matplotlib: A 2d graphics environment. *Computing in Science & Engineering*, 9(3):90–95, 2007.
- [64] S. Husa, S. Khan, M. Hannam, M. Pürrer, F. Ohme, X. J. Forteza, and A. Bohé. Frequency-domain gravitational waves from nonprecessing black-hole binaries. i. new numerical waveforms and anatomy of the signal. *Phys. Rev. D*, 93:044006, Feb 2016.
- [65] S. Husa, S. Khan, M. Hannam, M. Pürrer, F. Ohme, X. Jiménez Forteza, and A. Bohé. Frequency-domain gravitational waves from nonprecessing black-hole binaries. I. New numerical waveforms and anatomy of the signal. *Phys. Rev. D*, 93(4):044006, 2016.
- [66] K. Jani, J. Healy, J. A. Clark, L. London, P. Laguna, and D. Shoemaker. Georgia tech catalog of gravitational waveforms. *Classical and Quantum Gravity*, 33(20):204001, sep 2016.
- [67] P. Jaranowski and A. Królak. Gravitational-wave data analysis. formalism and sample applications: The gaussian case, 2007.
- [68] S. Khan, K. Chatziioannou, M. Hannam, and F. Ohme. Phenomenological model for the gravitational-wave signal from precessing binary black holes with two-spin effects. *Physical Review D*, 100(2), jul 2019.
- [69] S. Khan, S. Husa, M. Hannam, F. Ohme, M. Pürrer, X. J. Forteza, and A. Bohé. Frequency-domain gravitational waves from nonprecessing black-hole binaries. ii. a phenomenological model for the advanced detector era. *Phys. Rev. D*, 93:044007, Feb 2016.
- [70] S. Khan, F. Ohme, K. Chatziioannou, and M. Hannam. Including higher order multipoles in gravitational-wave models for precessing binary black holes. *Phys. Rev. D*, 101(2):024056, 2020.
- [71] A. Kolmogorov. Sulla determinazione empirica di una legge di distribuzione. *Inst. Ital. Attuari, Giorn.*, 4:83–91, 1933.
- [72] Kullback. *Information theory and statistics*. John Wiley and Sons, NY, 1959.
- [73] P. Landry and R. Essick. Nonparametric inference of the neutron star equation of state from gravitational wave observations. *Phys. Rev. D*, 99(8):084049, Apr. 2019.
- [74] J. Lange, R. O’Shaughnessy, and M. Rizzo. Rapid and accurate parameter inference for coalescing, precessing compact binaries, 2018.
- [75] N. Leslie, L. Dai, and G. Pratten. Mode-by-mode relative binning: Fast likelihood estimation for gravitational waveforms with spin-orbit precession and multiple harmonics. *Physical Review D*, 104(12), dec 2021.
- [76] F. Löffler, J. Faber, E. Bentivegna, T. Bode, P. Diener, R. Haas, I. Hinder, B. C. Mundim, C. D. Ott, E. Schnetter, G. Allen, M. Campanelli, and P. Laguna. The einstein toolkit: a community computational infrastructure for relativistic astrophysics. *Classical and Quantum Gravity*, 29(11):115001, may 2012.
- [77] S. Mastroianni, K. Leyde, C. Karathanasis, E. Chassande-Mottin, D. A. Steer, J. Gair, A. Ghosh, R. Gray, S. Mukherjee, and S. Rinaldi. On the importance of source population models for gravitational-wave cosmology. *Phys. Rev. D*, 104(6):062009, Sept. 2021.
- [78] S. Morisaki and V. Raymond. Rapid parameter estimation of gravitational waves from binary neutron star coalescence using focused reduced order quadrature. *Physical Review D*, 102(10), nov 2020.
- [79] A. H. Mroué, M. A. Scheel, B. Szilágyi, H. P. Pfeiffer, M. Boyle, D. A. Hemberger, L. E. Kidder, G. Lovelace, S. Ossokine, N. W. Taylor, A. Zenginoğlu, L. T. Buchman, T. Chu, E. Foley, M. Giesler, R. Owen, and S. A. Teukolsky. Catalog of 174 binary black hole simulations for gravitational wave astronomy. *Physical Review Letters*, 111(24), dec 2013.
- [80] A. Nagar et al. Time-domain effective-one-body gravitational waveforms for coalescing compact binaries with nonprecessing spins, tides and self-spin effects. *Phys. Rev. D*, 98(10):104052, 2018.
- [81] R. Narayan, T. Piran, and A. Shemi. Neutron Star and Black Hole Binaries in the Galaxy. 379:L17, Sept. 1991.
- [82] A. H. Nitz, C. D. Capano, S. Kumar, Y.-F. Wang, S. Kasta, M. Schäfer, R. Dhurkunde, and M. Cabero. 3-OGC: Catalog of gravitational waves from compact-binary mergers. *The Astrophysical Journal*, 922(1):76, nov 2021.
- [83] R. O’Shaughnessy, B. Farr, E. Ochsner, H.-S. Cho, C. Kim, and C.-H. Lee. Parameter estimation of gravitational waves from nonprecessing black hole-neutron star inspirals with higher harmonics: Comparing Markov-chain Monte Carlo posteriors to an effective Fisher matrix. *Phys. Rev. D*, 89(6):064048, Mar. 2014.
- [84] R. O’Shaughnessy, B. Farr, E. Ochsner, H.-S. Cho, V. Raymond, C. Kim, and C.-H. Lee. Parameter estimation of gravitational waves from precessing black hole-neutron star inspirals with higher harmonics. *Phys. Rev. D*, 89:102005, May 2014.
- [85] R. O’Shaughnessy and J. Lange. Code repository for RIFT: Rapid Iterative FITting for gravitational wave source parameter inference. Available at <https://git.ligo.org/rapidpe-rift/rift/>, 2015.
- [86] S. Ossokine, A. Buonanno, S. Marsat, R. Cotesta, S. Babak, T. Dietrich, R. Haas, I. Hinder, H. P. Pfeiffer, M. Pürrer, C. J. Woodford, M. Boyle, L. E. Kidder, M. A. Scheel, and B. Szilágyi. Multipolar effective-one-body waveforms for precessing binary black holes: Construction and validation. *Physical Review D*, 102(4), aug 2020.
- [87] S. Ossokine et al. Multipolar Effective-One-Body Waveforms for Precessing Binary Black Holes: Construction and Validation. *Phys. Rev. D*, 102(4):044055, 2020.
- [88] Y. Pan, A. Buonanno, A. Taracchini, L. E. Kidder, A. H. Mroué, H. P. Pfeiffer, M. A. Scheel, and B. Szilágyi. Inspiral-merger-ringdown waveforms of spinning, precessing black-hole binaries in the effective-one-body formalism. *Phys. Rev. D*, 89(8):084006, 2014.
- [89] C. Pankow, P. Brady, E. Ochsner, and R. O’Shaughnessy. Novel scheme for rapid parallel parameter estimation of gravitational waves from compact binary coalescences. *Phys. Rev. D*, 92:023002, Jul 2015.
- [90] E. Poisson and C. M. Will. Gravitational waves from inspiraling compact binaries: Parameter estimation using second-post-Newtonian waveforms. *Phys. Rev. D*,



52:848–855, July 1995.

- [91] G. Pratten, C. Garca a-Quiros, M. Colleoni, A. Ramos-Buades, H. Estelles, M. Mateu-Lucena, R. Jaume, M. Haney, D. Keitel, J. E. Thompson, and S. Husa. Computationally efficient models for the dominant and subdominant harmonic modes of precessing binary black holes. *Physical Review D*, 103(10), may 2021.
- [92] G. Pratten, S. Husa, C. Garcia-Quiros, M. Colleoni, A. Ramos-Buades, H. Estelles, and R. Jaume. Setting the cornerstone for a family of models for gravitational waves from compact binaries: The dominant harmonic for nonprecessing quasicircular black holes. *Phys. Rev. D*, 102(6):064001, 2020.
- [93] A. Ramos-Buades, S. Husa, G. Pratten, H. Estelles, C. Garca-Quiros, M. Mateu-Lucena, M. Colleoni, and R. Jaume. First survey of spinning eccentric black hole mergers: Numerical relativity simulations, hybrid waveforms, and parameter estimation. *Phys. Rev. D*, 101:083015, Apr 2020.
- [94] A. Ray, M. Camilo, J. Creighton, S. Ghosh, and S. Morisaki. Rapid Hierarchical Inference of Neutron Star Equation of State from multiple Gravitational Wave Observations of Binary Neutron Star Coalescences. *arXiv e-prints*, page arXiv:2211.06435, Nov. 2022.
- [95] S. Rinaldi and W. D. Pozzo. (h)DPGMM: a hierarchy of dirichlet process gaussian mixture models for the inference of the black hole mass function. *Monthly Notices of the Royal Astronomical Society*, 509(4):5454–5466, nov 2021.
- [96] J. Sadiq, T. Dent, and D. Wysocki. Flexible and fast estimation of binary merger population distributions with adaptive kde, 2021.
- [97] J. D. Scargle, J. P. Norris, B. Jackson, and J. Chiang. Studies in Astronomical Time Series Analysis. VI. Bayesian Block Representations. *Astrophysical Journal*, 764(2):167, Feb. 2013.
- [98] L. P. Singer and L. R. Price. Rapid bayesian position reconstruction for gravitational-wave transients. *Physical Review D*, 93(2), jan 2016.
- [99] J. Steinhoff, T. Hinderer, A. Buonanno, and A. Taracchini. Dynamical Tides in General Relativity: Effective Action and Effective-One-Body Hamiltonian. *Phys. Rev. D*, 94(10):104028, 2016.
- [100] C. Talbot, R. Smith, E. Thrane, and G. B. Poole. Parallelized inference for gravitational-wave astronomy. *Phys. Rev. D*, 100:043030, Aug 2019.
- [101] C. Talbot and E. Thrane. Fast, flexible, and accurate evaluation of gravitational-wave Malmquist bias with machine learning. *arXiv e-prints*, page arXiv:2012.01317, Dec. 2020.
- [102] A. Taracchini et al. Effective-one-body model for black-hole binaries with generic mass ratios and spins. *Phys. Rev. D*, 89(6):061502, 2014.
- [103] The LIGO Scientific Collaboration. GW190412: Observation of a binary-black-hole coalescence with asymmetric masses. *Physical Review D*, 102(4), aug 2020.
- [104] The LIGO Scientific Collaboration, the Virgo Collaboration, B. P. Abbott, R. Abbott, T. D. Abbott, S. Abraham, and et al. Population properties of compact objects from the second LIGO–Virgo Gravitational-Wave Transient Catalog. *Available as LIGO-P2000077*, Oct. 2020.
- [105] The LIGO Scientific Collaboration, the Virgo Collaboration, B. P. Abbott, R. Abbott, T. D. Abbott, and et al. Model comparison from LIGO–Virgo data on GW170817’s binary components and consequences for the merger remnant. *Classical and Quantum Gravity*, 37(4):045006, Feb. 2020.
- [106] V. Tiwari. VAMANA: modeling binary black hole population with minimal assumptions. *Classical and Quantum Gravity*, 38(15):155007, jul 2021.
- [107] V. Varma, S. E. Field, M. A. Scheel, J. Blackman, D. Gerosa, L. C. Stein, L. E. Kidder, and H. P. Pfeiffer. Surrogate models for precessing binary black hole simulations with unequal masses. *Physical Review Research*, 1(3), oct 2019.
- [108] V. Varma, S. E. Field, M. A. Scheel, J. Blackman, D. Gerosa, L. C. Stein, L. E. Kidder, and H. P. Pfeiffer. Surrogate models for precessing binary black hole simulations with unequal masses. *Physical Review Research*, 1(3), oct 2019.
- [109] J. Veitch, V. Raymond, B. Farr, W. Farr, P. Graff, S. Vitale, B. Aylott, K. Blackburn, N. Christensen, M. Coughlin, W. Del Pozzo, F. Feroz, J. Gair, C.-J. Haster, V. Kalogera, T. Littenberg, I. Mandel, R. O’Shaughnessy, M. Pitkin, C. Rodriguez, C. Rover, T. Sidery, R. Smith, M. Van Der Sluys, A. Vecchio, W. Vousden, and L. Wade. Parameter estimation for compact binaries with ground-based gravitational-wave observations using the lalinference software library. *Phys. Rev. D*, 91:042003, Feb 2015.
- [110] P. Virtanen, R. Gommers, T. E. Oliphant, M. Haberland, T. Reddy, D. Cournapeau, E. Burovski, P. Peterson, W. Weckesser, J. Bright, S. J. van der Walt, M. Brett, J. Wilson, K. J. Millman, N. Mayorov, A. R. J. Nelson, E. Jones, R. Kern, E. Larson, C. J. Carey, . Polat, Y. Feng, E. W. Moore, J. VanderPlas, D. Laxalde, J. Perktold, R. Cimrman, I. Henriksen, E. A. Quintero, C. R. Harris, A. M. Archibald, A. H. Ribeiro, F. Pedregosa, P. van Mulbregt, and SciPy 1.0 Contributors. SciPy 1.0: Fundamental Algorithms for Scientific Computing in Python. *Nature Methods*, 17:261–272, 2020.
- [111] C. K. Williams and C. E. Rasmussen. *Gaussian processes for machine learning*, volume 2. MIT press Cambridge, MA, 2006.
- [112] J. Wofford, A. Yelikar, H. Gallagher, E. Champion, D. Wysocki, V. Dellavero, J. Lange, C. Rose, S. Morisaki, and R. O’Shaughnessy. Expanding rift: Improving performance for gw parameter inference. 2022.
- [113] K. W. K. Wong and D. Gerosa. Machine-learning interpolation of population-synthesis simulations to interpret gravitational-wave observations: A case study. *Phys. Rev. D*, 100(8):083015, Oct. 2019.
- [114] D. Wysocki, D. Gerosa, R. O’Shaughnessy, K. Belczynski, W. Gladysz, E. Berti, M. Kesden, and D. E. Holz. Explaining LIGO’s observations via isolated binary evolution with natal kicks. *Phys. Rev. D*, 97(4):043014, Feb. 2018.
- [115] D. Wysocki, D. Gerosa, R. O’Shaughnessy, K. Belczynski, W. Gladysz, E. Berti, M. Kesden, and D. E. Holz. Explaining ligo’s observations via isolated binary evolution with natal kicks. *Physical Review D*, 97(4), Feb 2018.
- [116] D. Wysocki, J. Lange, and R. O’Shaughnessy. Reconstructing phenomenological distributions of compact binaries via gravitational wave observations. *Physical Re-*

- view D*, 100(4), Aug 2019.
- [117] D. Wysocki, R. O’Shaughnessy, L. Wade, and J. Lange. Inferring the neutron star equation of state simultaneously with the population of merging neutron stars, 2020.
- [118] B. Zackay, L. Dai, and T. Venumadhav. Relative binning and fast likelihood evaluation for gravitational wave parameter estimation, 2018.
- [119] M. ZILHÁ O and F. LÖFFLER. AN INTRODUCTION TO THE EINSTEIN TOOLKIT. *International Journal of Modern Physics A*, 28(22n23):1340014, sep 2013.